JCB Article

Pathology of a mouse mutation in peripheral myelin protein P0 is characteristic of a severe and early onset form of human Charcot-Marie-Tooth type 1B disorder

Annette E. Rünker,[1] Igor Kobsar,[2] Torsten Fink,[1] Gabriele Loers,[1] Thomas Tilling,[1] Peggy Putthoff,[1] Carsten Wessig,[2] Rudolf Martini,[2] and Melitta Schachner[1]

[1]Center for Molecular Neurobiology, University of Hamburg, D-20246 Hamburg, Germany
[2]Department of Neurology, Section of Developmental Neurobiology, Bayerische Julius-Maximilians University, D-97080 Würzburg, Germany

Mutations in the gene of the peripheral myelin protein zero (P0) give rise to the peripheral neuropathies Charcot-Marie-Tooth type 1B disease (CMT1B), Déjérine-Sottas syndrome, and congenital hypomyelinating neuropathy. To investigate the pathomechanisms of a specific point mutation in the *P0* gene, we generated two independent transgenic mouse lines expressing the pathogenic CMT1B missense mutation Ile106Leu (P0sub) under the control of the P0 promoter on a wild-type background. Both P0sub-transgenic mouse lines showed shivering and ultrastructural abnormalities including retarded myelination, onion bulb formation, and dysmyelination seen as aberrantly folded myelin sheaths and tomacula in all nerve fibers. Functionally, the mutation leads to dispersed compound muscle action potentials and severely reduced conduction velocities. Our observations support the view that the Ile106Leu mutation acts by a dominant-negative gain of function and that the P0sub-transgenic mouse represents an animal model for a severe, tomaculous form of CMT1B.

Introduction

The hereditary motor and sensory neuropathies are a clinically and genetically heterogeneous group of diseases of the peripheral nervous system of humans (Young and Suter, 2001, 2003). Among the different forms of these diseases is the Charcot-Marie-Tooth (CMT) type 1 neuropathy (Kamholz et al., 2000). CMT1 is characterized by distal muscle weakness and atrophy, reduced nerve conduction velocities, and de- and remyelination with onion bulb formation as observed in sural nerve biopsies (Dyck et al., 1993). Among the main forms of CMT1, CMT1B is caused by mutations in the major peripheral myelin protein zero (P0; Hayasaka et al., 1993a,c; Kulkens et al., 1993; Shy et al., 2002). Mutations in *P0* also give rise to severe disorders such as Déjérine-Sottas syndrome (DSS) and congenital hypomyelinating neuropathy (Hayasaka et al., 1993b; for reviews see Warner et al., 1996; Martini et al., 1998; Kamholz et al., 2000; Bennett and Chance, 2001; Shy et al., 2002).

P0 is a transmembrane recognition molecule that belongs to the Ig superfamily. It acts as a homophilic adhesion molecule involved in the formation and maintenance of the intraperiod and major dense lines that are instrumental in the compaction of myelin lamellae (Schneider-Schaulies et al., 1990; Martini, 1994; Martini et al., 1995a). Crystallographic analysis supports the notion that the extracellular domain of the molecule is involved in interdigitation of P0 tetramers on opposing myelin lamellae (Shapiro et al., 1996; Inoue et al., 1999). Experiments on the P0-deficient mouse indicate a role for P0 not only in myelin formation, but also in maintenance of myelin integrity (Martini and Schachner, 1997).

P0 null mutant mice have been considered as a model of patients with DSS that are homozygous for functional null mutations (Giese et al., 1992; Martini et al., 1995b;

A.E. Rünker and I. Kobsar contributed equally to this paper.

R. Martini and M. Schachner contributed equally to this paper.

Address correspondence to Melitta Schachner, Zentrum für Molekulare Neurobiologie, Universität Hamburg, Martinistr. 52, D-20246 Hamburg, Germany. Tel.: (49) 40-42803-6246. Fax: (49) 40-42803-6248. email: melitta.schachner@zmnh.uni-hamburg.de

A.E. Rünker's present address is Developmental Neurobiology, Department of Genetics, Smurfit Institute, Trinity College Dublin, Dublin 2, Ireland.

Key words: myelin P0 protein; myelin; peripheral neuropathies; tomacula; dominant-negative effects

Abbreviations used in this paper: CMT, Charcot-Marie-Tooth disease; DSS, Déjérine-Sottas syndrome; P0, peripheral myelin protein zero.

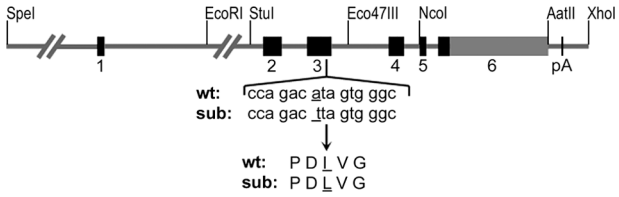

Figure 1. **Design of the P0sub-transgenic construct.** Shown is the localization of the substitution mutation within the P0 transgene and the changes (underlined) in comparison to the wild-type (wt) sequence at the level of nucleotides (in lowercase letters) or amino acids (in capital letters). The position of important restriction sites and their corresponding enzymes are indicated above the construct. Black boxes, exons; gray box, 3′ untranslated region of exon 6; pA, polyadenylation signal.

Warner et al., 1996). The heterozygous P0 null mutant mouse represents a late onset, milder neuropathy, and has been considered as a model for CMT1B patients carrying a loss of function mutation in one allele (Martini et al., 1995b; Martini, 1999). The majority of human *P0* mutations is heterozygous and causes a more severe phenotype than that of heterozygous P0-deficient mice. It has been suggested that these mutations act through gain of function (Hayasaka et al., 1993b; Kirschner and Saavedra, 1994). The possibility that some mutations may act through gain of function and others through loss of function could explain, at least to some extent, the findings that patients carrying mutations in the *P0* gene are either affected by the mild form of CMT1B or more severe forms of the disease (Martini et al., 1995b).

To develop a mouse model of a severe and early onset form of CMT1B, we have generated a transgenic mouse line with a substitution of isoleucine at residue 106 to leucine (P0sub; Gabreëls-Festen et al., 1996). This mutation in the human is characterized by the occurrence of many folded myelin profiles, termed tomacula, appearing as focally thickened myelin passing into thinner myelin sheaths within the same internode. Fibers outside tomacula are frequently devoid of myelin or are thinly (re)myelinated. Onion bulbs are composed of thin Schwann cell layers and contain many double basement membranes. Uncompacted myelin is encountered only in few fibers. Here, we report that transgenic mice expressing this point mutation in conjunction with the two endogenous wild-type P0 alleles show a similar phenotype, including severe muscle weakness, hypomyelination, tomacula formation, and low conduction velocities, as well as retarded and arrested myelin development.

The combined observations support the view that the Ile106Leu mutation acts by dominant-negative gain of function and that the P0sub-transgenic mice represent the first authentic model for the severe and early onset form of tomaculous CMT1B in humans.

Results

Transgenic mice expressing the P0 substitution mutation show motor abnormalities

An A→T nucleotide exchange was introduced into exon 3 of the *P0* gene to express the pathogenic P0 missense mutation Ile106Leu (Gabreëls-Festen et al., 1996) under the control of the P0 promoter in addition to endogenous P0 expression. The expression construct (termed P0sub; Fig. 1) included 6 kb of 5′ flanking sequence, all exons and introns, and the natural polyadenylation signal (Feltri et al., 1999). The P0 promoter was previously shown to regulate the expression of lacZ in parallel with the endogenous P0 promoter during postnatal development and after Wallerian degeneration (Feltri et al., 1999), and to produce structurally normal myelin when P0 was expressed in $P0^{-/-}$ mice (Wrabetz et al., 2000).

We produced two founder P0sub mouse lines (P0sub1 and P0sub3) which transmitted the transgene to their offspring. The transgenic mice of both lines shivered dramatically and showed different signs of muscle weakness pronounced from the fourth week onwards. For example, when placed on a pole they were either not able to grab the pole with their hindlimbs or slipped down if they tried to grab the pole. In addition, the transgenic mice frequently dragged their paws while walking and clenched their paws while hanging at their tails. The transgenic males were not able to breed, most likely due to impaired motor abilities.

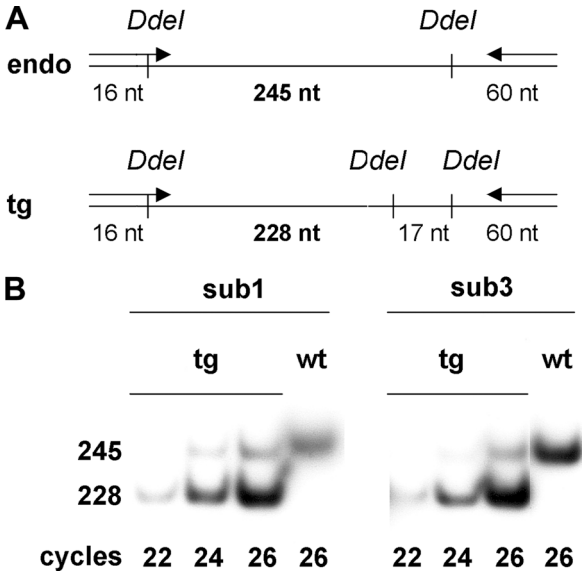

Figure 2. **RT-PCR analysis demonstrates overexpression of the transgene in P0sub mice.** (A) Total RNA prepared from sciatic nerve was reverse transcribed; the product was amplified by PCR using a primer pair that recognized identically both endogenous (endo) and transgenic (tg) P0 cDNAs. The tg cDNA could be distinguished from the endo cDNA by DdeI digestion, yielding a tg-specific fragment of 228 nt and an endo-specific fragment of 245 nt. (B) Reverse-transcribed products from sciatic nerve total RNA of 6-wk-old transgenic (tg) P0sub1 and P0sub3 mice were analyzed for the relative proportions of transgenic and endogenous P0 mRNA. In both lines, an overexpression of transgenic mRNA was observed. Note that for cDNA from wild-type (wt) littermates used as a control, only the 245-nt band was detected, confirming the specificity of the 228-nt band for transgenic P0 cDNA. Aliquots of different PCR cycle numbers (22, 24, and 26) were analyzed in order to ensure that only the logarithmic phase of PCR was considered for quantification. The P0sub3-transgenic samples and the corresponding wild-type control were grouped from different parts of the same gel for reasons of space (film exposure was identical).

Table I. **P0 transgenic mRNA is overexpressed relative to endogenous mRNA in P0sub mice**

Mouse line	P0sub1	P0sub3
Fold overexpression of transgenic mRNA	6.0 ± 0.3	6.1 ± 0.7

Mice were 42 d old; $n = 4$ for both lines; values are given as mean ± SD.

The transgenic P0 mRNA is overexpressed compared with the endogenous P0 transcripts in P0sub mice

To determine the ratio between transgenic and endogenous P0 message in P0sub mice, we used an RT-PCR assay based on a method described by Feltri et al. (1999), exploiting a DdeI site present in the sub transgene, but not in the endogenous *P0* (Fig. 2 A). After DdeI digestion of RT-PCR products from sciatic nerves, a 228-nt band, corresponding to the transgenic message, was observed in all samples from transgenic mice, and appeared more intense than a 245-nt band representing the endogenous P0 mRNA (Fig. 2 B). The 228-nt band was specific, as omission of reverse transcription product did not produce any bands (unpublished data), and DdeI digestion of RT-PCR product from wild-type animals only yielded the 245-nt band (Fig. 2 B). Densitometry revealed that in P0sub1 and P0sub3 mice, the transgenic P0 mRNA is approximately sixfold overexpressed relative to the endogenous P0 mRNA (Table I).

P0 protein is not overexpressed in myelin of P0sub mice

The content of P0 within peripheral nerves was estimated by immunoblot analysis of total nerve homogenates (Fig. 3, A and B). The P0-immunoreactive bands of transgenic mice in the founder lines P0sub1 (Fig. 3 A) and P0sub3 (Fig. 3 B) were decreased by ~10-fold when compared with equal protein amounts of wild-type mice (Table II). This finding might reflect the strong hypomyelination observed in peripheral nerves (see below), but does not relate to the amount of P0 protein incorporated into myelin.

To investigate if the abnormal phenotype of P0sub mice is the result of an overexpression of P0 protein in myelin, we characterized the myelin fraction of peripheral nerve homogenates by immunoblot analysis (Fig. 3, C and D). We obtained different results for the two founder lines: although the amount of P0 in the myelin fraction of P0sub1-transgenic mice (Fig. 3 C) was reduced by approximately fivefold compared with wild-type mice, the P0sub3-transgenic mice (Fig. 3 D) showed a P0 content in the range of that seen in wild-type mice (Table II). These data exclude the possibility that an over- or underexpression of P0 protein in peripheral

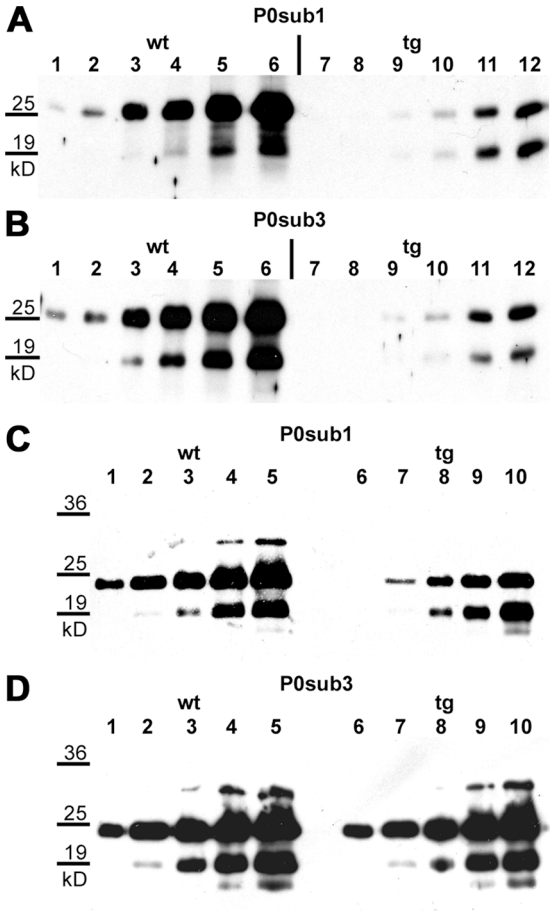

Figure 3. **P0 immunoblot analysis of total and myelin fraction of peripheral nerve homogenates of wild-type and P0sub mice.** (A and B) In immunoblots of total nerve homogenates, the intensities of the P0-immunoreactive bands of the P0sub1- and P0sub3-transgenic mice are dramatically reduced (~10 times) compared with wild-type mice. This accounts for the low content of myelin in the sciatic nerves of the transgenic animals. (C and D) Although the amount of P0 protein within peripheral myelin of P0sub3-transgenic mice is comparable to that of wild-type mice (D), the P0 content is significantly reduced in myelin isolated from transgenic mice of P0sub1 (C). Different amounts of protein were applied (for A and B): lanes 1 and 7, 0.1 μg; lanes 2 and 8, 0.2 μg; lanes 3 and 9, 0.5 μg; lanes 4 and 10, 1 μg; lanes 5 and 11, 2 μg; lanes 6 and 12, 5 μg; and (for C and D): lanes 1 and 6, 0.01 μg; lanes 2 and 7, 0.05 μg; lanes 3 and 8, 0.1 μg; lanes 4 and 9, 0.25 μg; lanes 5 and 10, 0.5 μg. P0 protein was detected with polyclonal P0 (A and B) or monoclonal P07 (C and D) antibody.

Table II. **P0 protein expression in P0sub-transgenic mice relative to wild-type littermates**

Mouse line	P0sub1		P0sub3	
	Wild-type mice	Transgenic mice	Wild-type mice	Transgenic mice
Expression of P0 protein in sciatic nerve homogenate[a]	1.00 ± 0.29	0.12 ± 0.05	1.00 ± 0.10	0.09 ± 0.04
Expression of P0 protein in myelin fraction[a]	1.00 ± 0.48	0.21 ± 0.03	1.00 ± 0.65	1.04 ± 0.70

[a]Average P0 protein level in wild-type animals was set to 1; mice were 56 d old; $n = 3$ for both lines; values are given as mean ± SD.

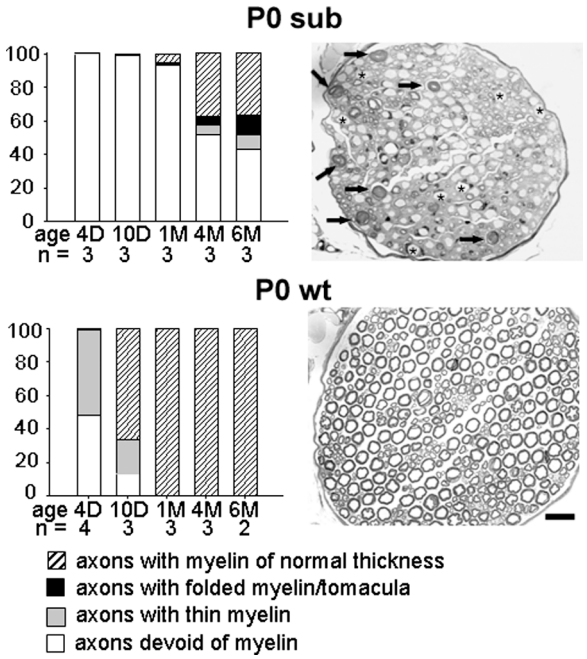

Figure 4. **P0sub causes impaired myelin development, myelin arrest, and tomaculous abnormalities.** Left side: EM-based morphometric analysis of femoral quadriceps nerves of developing (4 d, 10 d, and 1 mo) and adult (4 and 6 mo) P0sub1 and P0 wt mice. The numbers of the distinct morphological profiles (e.g., the "number of axons with myelin of normal thickness") are given as percentage values of the total axon number of the femoral nerve (~550). "n" indicates the number of mice used for a respective age. Right side: representative semi-thin sections of femoral quadriceps nerves of 6-mo-old P0sub1 mutants and wt mice, reflecting the strongly impaired myelin formation in the mutants. Arrows indicate tomacular profiles in the mutant, asterisks nonmyelinated axons of larger caliber. More pathological details are given in Fig. 5. Bar in the bottom micrograph (for both micrographs) is 20 μm.

myelin may cause the abnormal phenotype of P0sub-transgenic mice.

Light microscopic and ultrastructural abnormalities in the peripheral nervous system of the P0sub-transgenic mice

adult stage. To obtain quantitative histopathological data, we investigated the two major branches of the femoral nerve of P0sub1 and P0sub3 mice, comprising the motor quadriceps and cutaneous saphenous nerve, by EM. The quadriceps nerve contains ~550 myelinated axons that are predominantly of larger caliber, whereas the saphenous branch comprises ~650 myelinated axons of predominantly smaller caliber (Lindberg et al., 1999). In addition, and as opposed to the quadriceps nerves, unmyelinated nerve fibers are abundant in the saphenous branch.

In 6-mo-old wild-type mice, the two major branches of the femoral nerves were completely myelinated. However, in both lines of the transgenic mice, myelination was severely impaired in both branches of the femoral nerve, but axon numbers were not significantly reduced in these nerves (568 ± 14.8 in the mutants and 554 ± 16.7 in wild types; $P > 0.3$). The typical pathological profiles in the cross-sectioned femoral nerves were abnormally folded myelin profiles and myelin thickenings of normal compaction (~12 and 10% of all axonal profiles of lines P0sub1 and P0sub3, respectively; Fig. 4 and Fig. 5). In the following, we designate these abnormalities as tomacula. In addition, abnormally thinly myelinated profiles (~9 and 10% in P0sub1 and P0sub3, respectively) or axons completely devoid of myelin (43 and 48% in P0sub1 and P0sub3, respectively) were abundant (Fig. 4 and Fig. 5 A). Furthermore, supernumerary Schwann cells in the form of onion bulbs were frequently seen (Fig. 5 A). These abnormal features were also seen in sciatic nerves (Fig. 5 C) and spinal roots (Fig. 5 D), and are highly reminiscent of those described for sural nerve biopsies from a CMT1B patient carrying the same P0 mutation as the transgenic mice (Gabreëls-Festen et al., 1996).

As a next step, we investigated single-fiber preparations from quadriceps nerves of both wild-type and mutant mice. In wild-type mice, myelin sheaths were regularly shaped with nodes of Ranvier forming the borders of apposing sheaths (Fig. 5 E). By contrast, in both transgenic lines, all fibers prepared were of abnormal appearance (50 fibers from 2 different mutant mice of each line). Each of the fibers showed tomacular swellings that were either internodal or at a paranodal position (Fig. 5 F). In addition, and in support of the electron microscopic analyses, the aspects not associated with tomacula showed much thinner myelinated profiles than those of wild-type mice, or lacked myelin completely.

Electrophysiological investigations of adult mice of the P0sub1 line revealed a robust reduction of amplitudes of compound muscle action potentials of plantar muscles from 12.8 mV (±2.9 mV) in wild-type mice to 1.1 mV (±0.19 mV) in the mutants. Mean nerve conduction velocity was reduced from 40.2 m/s (± 2.9 m/s) to 2.0 m/s (± 0.3 m/s, $P < 0.001$) with dispersed response. F-wave latency could not be recorded at this age (Fig. 6), but in 2-mo-old mutants, a dramatically prolonged F-wave (4.7 ± 0.4 ms in wild-type mice vs. 48 ± 5.5 ms in the mutants, $P < 0.001$) could be recorded. Similar values were obtained from line P0sub3 (unpublished data).

Developmental stages. To investigate whether the severe myelinopathy of the transgenic mice developed at onset of myelination or was the result of myelin degeneration, we investigated the quadriceps branch of the femoral nerve of wild-type and transgenic mice at 4 and 10 d, and at 1 and 4 mo of age.

In 4-d-old wild-type mice, ~50% of the fibers of the quadriceps nerve showed myelin sheaths that were all of thin appearance (Fig. 4). In 10-d-old mice, almost all fibers were myelinated, including myelin sheaths of normal and low thickness (Fig. 4). During the following stages, all myelinated fibers of the wild-type mice increased in diameter and achieved their final size at 4 mo.

In both mutant lines, there was no detectable myelin at postnatal d 4 and only very few fibers showed myelinated aspects at postnatal d 10 (Fig. 4). At 1 mo after birth, three groups of myelinated fibers were detectable comprising visually normal myelin, myelin tomacula, and abnormally thin myelin (Fig. 4). These myelin-like sheaths constantly increased in number up to 6 mo after birth, the oldest stage investigated. In spite of this increase, ~43 and 48% of the nerve fibers of P0sub1 and P0sub3, respectively, remained

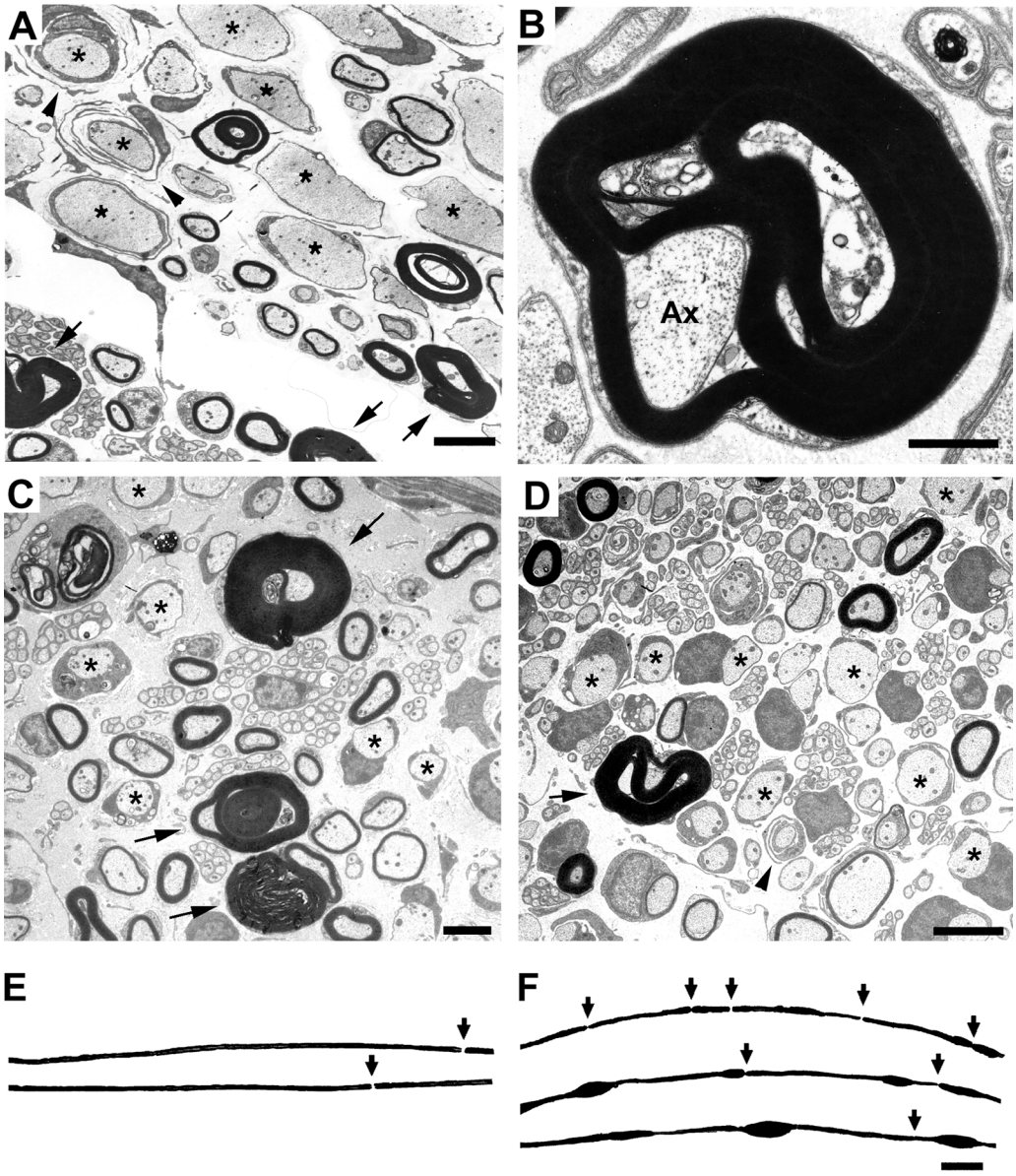

Figure 5. **P0sub causes a tomaculous neuropathy with impaired myelin formation in peripheral nerves.** Electron micrographs of femoral quadriceps nerves (A and B), sciatic nerves (C), and dorsal spinal roots (D) of adult P0sub1 mutants and single-fiber preparations from sciatic nerves of adult wild-type (E) and P0sub1 mutants (F). (A) Low power overview of a femoral quadriceps nerve of a P0sub1 mutant. Note tomacula (arrows), onion bulbs (arrowheads), and nonmyelinated axons of large caliber (asterisks) as typical pathological features. (B) High power EM of a tomaculum in the femoral quadriceps nerve of a P0sub1 mutant. Note folded and unusually thick myelin that displays normal compaction. Ax, axon. (C and D) Low power overviews of a sciatic nerve and a dorsal spinal root of a P0sub1 mutant. Note similar neuropathic hallmarks as seen in the femoral nerve. Arrows, tomacula; arrowheads, onion bulbs; asterisks, nonmyelinated large caliber axons. (E and F) Single-fiber preparations from wild-type (E) and P0sub1 mutant (F) mice. Note frequent tomacula in the mutants and absence of tomacula in the wild types. Arrows indicate nodes of Ranvier. Bars: 5 μm (A, C, and D), 1 μm (B), and 40 μm (F, for E and F).

unmyelinated (see above and Fig. 4). It is of note that the developing Schwann cells of the mutant showed an abnormal cytological appearance in that many of them contained abundant cytoplasmic myelin ovoids (unpublished data).

Discussion

The phenotype of P0sub mutants is caused by a P0 missense mutation

To develop an authentic mouse model for one severe and early onset form of CMT1B, we have generated two independent transgenic mouse lines expressing the pathogenic CMT1B missense mutation Ile106Leu (Gabreëls-Festen et al., 1996) under the control of the P0 promoter (Feltri et al., 1999) on a wild-type genetic background. Both P0sub mouse lines showed severe impairment of their motor abilities with remarkable muscle weakness. Morphological investigation of peripheral nerves of these mice revealed a severe myelinopathy that includes features of early onset dysmyelination, such as prominent hypomyelination and tomacula formation in all nerve fibers. These characteristics are very similar to the pathological phenotype of the severely affected

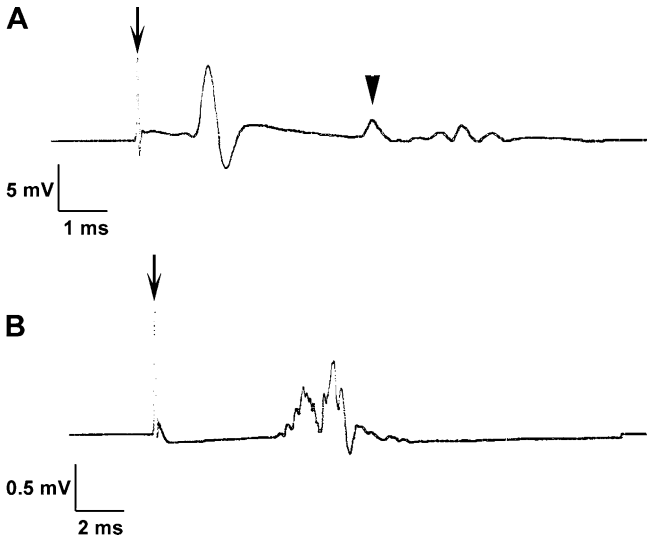

Figure 6. **Representative traces of nerve conduction experiments with distal stimulation of the tibial nerve of 6-mo-old mice at the ankle and needle electrode recording from intrinsic foot muscles.** (A) Normal amplitude of 11.0 mV and normal latency of 1.1 ms in the wild-type animal; normal F-wave response is depicted by arrowhead. (B) In the P0sub mutant (P0sub1), there is a disperse, polyphasic potential of only 1.0 mV; latency is prolonged to 5.2 ms (note different scales of time and amplitude axis). Arrows (in A and B) show stimulus artifact.

CMT1B patient that has initially been described as suffering from a congenital demyelinating motor and sensory neuropathy (Gabreëls-Festen et al., 1990). Later on, when genetic analyses were available, this patient was identified to carry an Ile106Leu substitution mutation in the *P0* gene and was classified as a CMT1B patient (Gabreëls-Festen et al., 1996). Electrophysiologically, we found strongly reduced nerve conduction velocities of only 2 m/s that again reflect the severe phenotype of the aforementioned patient displaying conduction velocities of 7 m/s. In our P0sub mutants, we observed a strong retardation and partial arrest of the myelination process during development, which is again in line with the pathological features of the aforementioned patient, whose pathological abnormalities have been identified at early childhood (Gabreëls-Festen et al., 1990, 1996).

We investigated the relative expression of transgenic and endogenous P0 message in P0sub mice and found that in P0sub1 and P0sub3 mice, the transgenic P0 mRNA is approximately sixfold overexpressed relative to the endogenous P0 mRNA. It is of note that a comparably high overexpression of the full-length *P0* transgene (approximately by factor 7 in the mutant Tg80.2) containing the *P0* wild-type gene leads to severe dysmyelination characterized by impaired axon sorting and arrest of myelin formation at the promyelin stage (Wrabetz et al., 2000; Yin et al., 2000). The dysmyelinating neuropathy in our model is strikingly different from that observed in the P0-overexpressing Tg80.2 mutants because impaired sorting and persistence of axon bundles of larger calibers were never observed in our P0sub mice. In addition, P0 protein is not overexpressed in the myelin fraction of adult P0sub mutants, whereas P0 protein was overexpressed in the adult Tg80.2 mutant by a factor of ~1.4 as evaluated by quantitative immuno-EM of the few myelin structures that were detectable in the transgenic overexpressors (Yin et al., 2000). Most importantly, both the P0sub1 and the P0sub3 lines developed tomaculous myelin structures in all peripheral nerve fibers, although the P0 protein levels differed by a factor of ~5 in the myelin fractions from the two sublines and never exceeded those of wild-type littermates. Occurrence of tomacula cannot be explained by the overexpression of P0 transcripts because tomacula have never been observed in transgenic mice overexpressing P0 (Wrabetz et al., 2000; Yin et al., 2000). Another transgenic mutant developed in our laboratory in parallel with P0sub1 and P0sub3, which expresses a human P0 mutation causing a DSS, does not produce myelin tomacula either, but is characterized by reduced myelin thickness (unpublished data). Therefore, we conclude that tomacula formation and most probably also the observed arrested myelination is a unique feature of P0sub1 and P0sub3 mice reflecting the effects of the substitution mutation.

The P0sub mutation is consistent with a dominant-negative gain of function

The most common features of CMT1B are hypo- and demyelination, combined with onion bulb formation. However, based on additional neuropathological features, two divergent forms of the disorder have been described (Gabreëls-Festen et al., 1996). The first form is characterized by the frequent occurrence of uncompacted myelin (~20–70% of myelinated fibers), whereas tomacula are almost absent (<1%). These features are most similar to the phenotype of heterozygous P0-deficient mice (Martini et al., 1995b), which thus express the characteristic features of these forms of CMT1B. The pathology of the other type of CMT1B, including the phenotype associated with the Ile106Leu substitution, is dominated by the abundant occurrence of tomacula and a lack of uncompacted myelin (<1%; Gabreëls-Festen et al., 1996). To date, tomaculous forms of CMT1B are described for six further point mutations: Ile33Phe, Ser49Leu, Lys67Glu, Asn93Ser, Lys101Arg, and Asn102Lys (Thomas et al., 1994; Gabreëls-Festen et al., 1996; Tachi et al., 1997; Nakagawa et al., 1999; Sindou et al., 1999; Fabrizi et al., 2000), of which the molecular pathology is unknown and which remain to be investigated in transgenic mouse models. We have shown that, in the presence of two P0 wild-type alleles, the P0sub-transgenic mice develop the same abnormal features and pathological characteristics as the human mutation Ile106Leu, which is a conservative amino acid substitution. It is worth mentioning in this context that this abnormal phenotype is not caused by a functional ablation of the mutant P0 allele in the sense that it causes a null mutation because heterozygous P0-deficient mice show normal development and maintenance of myelin until 4 mo of age, after which they display decompaction and degeneration of myelin. P0sub-transgenic mice, by contrast, show a severe and early onset dysmyelination, accompanied by the formation of tomacula in the absence of myelin decompaction. Thus, our results strongly suggest that the pathological phenotype of tomacula in P0sub-transgenic mice is the result of a dominant-negative gain of function effect of P0 protein that can impair the normal function of P0.

With regard to the developmental aspect of our work, we cannot rule out that the severe phenotype of the two P0sub-transgenic mouse lines is partially due to an overexpression of the mutant protein during development, possibly leading to an increased instability of the protein, as seen previously for P0 wild-type protein when transgenically overexpressed on a wild-type background (Wrabetz et al., 2000; Yin et al., 2000). However, we consider this possibility as sole cause for the impaired myelin development as unlikely. First, as mentioned above, the dysmyelinating phenotype in our mutants is different from and less severe than that of the Tg80.2 mutant studied by Wrabetz et al. (2000). Second, the frequent profiles of dysmyelinated fibers in the biopsies from the Ile106Leu patient are in line with the view that the mutation not only causes tomacula formation, but also impairs myelin formation as seen in the P0sub mice. Third, tomacula formation occurs in both P0sub lines independently of the amount of P0 protein expression in the myelin fraction. This argues that not the levels of the combined mutant and wild-type P0 proteins determine the characteristic features of the resultant mouse lines, but that the tomacula seen in the two independent founder P0sub-transgenic mice are the true consequence of this mutation. Thus, our P0sub-transgenic mice represent an animal model of the severe tomaculous form of the human mutation, as originally described by Gabreëls-Festen et al. (1996).

The question of whether this mutation also leads to abnormal expression of other proteins involved in myelination, such as PMP22, MAG, and periaxin, which produce tomacula (Rebai et al., 1989; Adlkofer et al., 1995, 1997; Carenini et al., 1997; Suter and Nave, 1999; Gillespie et al., 2000; Boerkoel et al., 2001; Cai et al., 2001, 2002; Guilbot et al., 2001; Takashima et al., 2002), remains presently unanswered. Tomacula are formed by homo- and heterozygous deletions of the *PMP22* gene and the homozygous ablations of the myelin-associated glycoprotein MAG and periaxin. Because some of these molecules have been shown to interact with each other, such as P0 with PMP22 (D'Urso et al., 1999), and because dysregulations of a substantial set of myelin proteins in the peripheral nervous system of mutant mice deficient in a particular myelin protein have been repeatedly observed (Martini and Schachner, 1997; Menichella et al., 2001), it is possible that dysregulation in expression of the proteins so far recognized as causing tomacula may indicate a common mechanism of molecular pathology. The mechanism underlying the complex network of interdependent synthesis, degradation, and subcellular localization of the individual myelin proteins that may be affected by a mutation in one gene will remain to be investigated to allow a molecular interpretation of the abnormal phenotypes in patients affected by P0 mutations. The availability of the first mouse model carrying the human P0 mutation causing tomacula is an important step toward elucidating these mechanisms.

Materials and methods

Generation of P0sub-transgenic mice

To generate a mouse mutant expressing the pathogenic substitution P0 Ile106Leu (P0sub; Gabreëls-Festen et al., 1996; Fig. 1) under the control of the P0 promoter (Feltri et al., 1999), the 2.6BsrGIsense vector, containing a 2.6-kb BsrGI fragment with exons 2–5 of the mouse P0 genomic DNA, was used for mutagenesis. The adenine at bp 1644 (ATG start codon in the genomic DNA as bp 1) was substituted to thymine using the Seamless PCR cloning kit (Stratagene) according to the manufacturer's protocol. In brief, the whole vector was amplified with primers flanking and containing the mutation and was re-ligated. A StuI–Eco47II fragment encoding exon 2 and mutated exon 3 of the resulting 2.6BsrGIsense-P0sub vector was cloned into the mP05.7blue vector (Lemke et al., 1988; Feltri et al., 1999), containing exons 2–6. Finally, an EcoRI fragment of the vector mP0Ewtblue (You et al., 1991; Feltri et al., 1999) comprising the P0 promoter and exon 1 was inserted into the EcoRI-digested mP05.7blue-P0sub vector.

The resulting transgenic constructs were verified by sequence analysis, and 12.3-kb fragments were excised from the vectors using SpeI and XhoI. The transgenes were microinjected into Friend virus B-type susceptibility (FVB) zygotes using standard techniques (Hogan et al., 1994). Three P0sub founder mice were identified by PCR and were crossed with wild-type FVB mice. Breeding lines of two P0sub founders (called P0sub1 and P0sub3) were crossed to FVB mice.

RT-PCR

Sciatic nerves were dissected from 6-wk-old P0sub1- and P0sub3-transgenic mice and from the respective wild-type littermates. Total RNA was prepared using the RNeasy Lipid Tissue kit (QIAGEN) according to the manufacturer's instructions. To analyze transgene relative to endogenous P0 expression, we used a modified version of the protocol described by Feltri et al. (1999). For this purpose, we exploited the A→T point mutation responsible for the Ile106Leu amino acid exchange. In brief, 200 ng total RNA was reverse transcribed using Moloney Murine Leukemia Virus Reverse Transcriptase (Promega) and random hexanucleotide primers (Amersham Biosciences). Equal volumes of the reverse-transcribed product from sciatic nerves of transgenic and wild-type animals were amplified in the presence of $\alpha[^{32}P]$dATP, using a single primer pair recognizing P0 exon 2 (5′-GTCCAGTGAATGGGTCTCAG-3′) and exon 4 (5′-GCTCCCAACACCACCCCATA-3′) that flanks a DdeI site present in the P0sub transgenes only. PCR conditions were: initial enzyme activation at 95°C for 15 min; followed by cycles consisting of 94°C for 30 s, 63°C for 60 s, and 72°C for 60 s; and a final extension step at 72°C for 10 min, in a standard PCR reaction mix containing HotStarTaq DNA polymerase (QIAGEN). To avoid the formation of heteroduplexes between the PCR products containing the additional DdeI site and those lacking this site, only cycles in the logarithmic range were chosen. Unincorporated nucleotides were removed from the RT-PCR products using Micro Bio-Spin P-30 columns (Bio-Rad Laboratories) according to the manufacturer's instructions. 4 μl of the purified RT-PCR products was digested with DdeI (New England Biolabs) at 37°C for 90 min. DNA fragments were resolved by PAGE and visualized both by phosphorimaging and by autoradiography. Intensity of the bands was quantified by densitometry of phosphorimager signals (Fujix BAS 2000; Fuji) using TINA 2.09 software (Raytest), and the ratio between the transgene-specific 228-bp fragment and the endogene-specific 245-bp fragment was calculated. To correct for the difference in incorporated dATPs, this intensity ratio was multiplied by a correction factor (1.063), yielding the transgenic P0 message/endogenous P0 message ratio.

Preparation of sciatic nerve homogenates and immunoblot analysis

The sciatic nerves of 2-mo-old wild-type and transgenic mice were homogenized in lysis buffer (20 mM Tris-HCl, pH 7.5, 150 mM NaCl, 1 mM EDTA, 1 mM EGTA, 1% NP-40, and 1× Complete® protease inhibitor cocktail [Roche]) and incubated at 4°C for 30 min. The homogenates were cleared by centrifugation three times at 12,000 *g* at 4°C for 20 min. The protein concentrations of homogenates were determined using the BCA Protein Assay kit (Pierce Chemical Co.). The samples were denatured in 5× sample buffer (10% glycerol, 5% β-mercaptoethanol, 5% SDS, and 0.1% bromophenol blue) at 95°C for 5 min and subjected to SDS-PAGE and immunoblot analysis using monoclonal (P07; 1:1,000 diluted; a gift of Dr. Juan Archelos; Archelos et al., 1993) or polyclonal (1:750 diluted) P0 antibodies. Primary antibodies were detected with HRP-conjugated anti–rat or anti–rabbit IgG (Dianova), and were visualized with ECL chemiluminescent substrate (Amersham Biosciences). For the quantification of films (BioMax; Kodak), images were captured by high resolution (600 × 600 dpi) 8-bit (256 gray level) microdensitometry with a flat-bed scanner (Arcus II; Agfa). The images were analyzed for optical density of bands using image analysis software (GelWorks 1D; Ultra-Violet Products). To determine the ratio between P0 expression in transgenic animals and P0 expression in wild-type animals, intensities of the main P0-immunoreactive band (25 kD) were measured in lanes loaded with different amounts of total protein (see Fig. 3) and were normalized to the total protein amount.

Myelin preparation

8-wk-old mice (5 wild-type and 15 transgenic animals for each mouse line) were anaesthetized using pentobarbital (Narcoren®) and subsequently perfused with PBS for 3–5 min in order to remove blood from peripheral nerves. Sciatic nerves, femoral nerves, and dorsal roots were prepared and frozen in liquid nitrogen. For homogenization, the nerves were mixed with ice-cold homogenization buffer (5 mM Tris-HCl, pH 7.4, 1 mM $NaHCO_3$, and 320 mM sucrose) and homogenized in a Potter homogenizer. The homogenate was centrifuged at 100 *g* and 4°C for 10 min. After this centrifugation step, the pellet and the supernatant were collected. The pellet was resuspended in homogenization buffer, and supernatant and homogenized pellet were applied on top of the first step sucrose gradient (320 mM – 650 mM – 1 M – 1.2 M). The gradients were centrifuged at 100,000 *g* and 4°C for 1 h. The interface between the 320-mM and 650-mM sucrose solution was collected, diluted with homogenization buffer, and centrifuged again for 20 min at 100,000 *g*. The resulting pellets were osmotically shocked and treated with 5 mM Tris-HCl, pH 8.3, for 45 min on ice. Afterwards, the samples were centrifuged at 100,000 *g* and 4°C for 20 min. The pellets were suspended in 5 mM Tris-HCl, pH 8.3, and applied to the top of a second sucrose step gradient (0 mM – 650 mM – 850 mM – 1 M – 1.2 M). The gradient was centrifuged at 100,000 *g* and 4°C for 1 h. The myelin fraction was collected at the 0 – 650 mM sucrose interface, washed in ice-cold PBS, and centrifuged for 30 min at 100,000 *g*. The resulting pellet was suspended in PBS and frozen at −80°C. Protein content of the samples was determined and immunoblot analyses were performed as described (see above).

Preservation of tissue for light and electron microscopy

Femoral and sciatic nerves were processed for light and electron microscopy as reported earlier (Carenini et al., 2001). The mice were transcardially perfused using 4% PFA and 2% glutaraldehyde in 0.1 M cacodylate buffer (pH 7.4). The nerves stayed in the same fixative overnight, followed by osmification and embedding in Spurr's medium.

For light microscopic analysis, 0.5-μm-thick semi-thin sections from femoral nerves were stained with alkaline methylene blue and were investigated with a light microscope (Axiophot; Carl Zeiss MicroImaging, Inc.) using a 40× objective. For EM, ultrathin sections of 70-nm thickness were counterstained with lead citrate and investigated using an electron microscope (model EM 10B; Carl Zeiss MicroImaging, Inc.). Primary magnification was between 2,500 and 25,000.

Morphometry

The quantitative analysis of pathological changes was performed on ultrathin sections using a BioVision slow scan camera attached to the Zeiss EM 10B microscope and using the corresponding software analySIS 3.0 Doku (Soft Imaging Systems). The following morphological parameters were assessed: axons with myelin of normal thickness, axons with thin myelin, axons with folded myelin/tomacula, and myelin-competent axons (larger than 1 μm in diameter) devoid of myelin. For the determination of relative myelin thickness, the g-ratio (a reciprocal measure of myelin thickness; Friede, 1972), was determined as recently described (Kobsar et al., 2003).

Statistical analysis

Comparison of the pathological features of the different genotypes was done by use of a Mann-Whitney-U test and statistical significance was defined for $P < 0.05$. Statistical analysis of the data was performed by use of Excel (Microsoft) and SYSTAT (SPSS, Inc.). Graphs were made using SigmaPlot 2001 (SPSS, Inc.).

Single-fiber preparations

Preparation of single nerve fibers was performed according to Martini et al. (1995b). In brief, sciatic nerves of transcardially perfused mice (see earlier in the Materials and methods) were removed and connective tissue around the nerves was stripped off, followed by gentle "pre-teasing" of fiber bundles. After osmification of fiber bundles and dehydration with acetone, single-fiber preparation was performed in nonpolymerized Spurr's medium using no. 5 watchmaker's forceps. Single fibers were transferred into a droplet of Spurr's medium on a slide, followed by cover-slipping and polymerization at 60°C. Light microscopy was performed with an Axiophot light microscope (Carl Zeiss MicroImaging, Inc.) using a 40× objective.

Electrophysiological measurements

Nerve conduction experiments of sciatic nerves from 4- and 6-mo-old mice were performed by established electrophysiological methods as described previously (Zielasek et al., 1996). In brief, after anesthesia the compound muscle action potential was recorded with two needle electrodes in the foot muscles after distal stimulation of the tibial nerve, one main branch of the sciatic nerve at the ankle, and proximal stimulation of the sciatic nerve at the sciatic notch. In all experiments, the investigator was not aware of the genotype. Statistical analysis was performed using a one-tailed *t* test for grouped data.

The authors are grateful to Dr. Michael Bösl for microinjection and transplantation of zygotes, to Dr. Marius Ader and Dr. Astrid Rollenhagen for help with preparation of nerves, to Dr. Laura Feltri for providing us with P0 vector constructs and for helpful suggestions and discussions, to Dr. Uwe Borgmeyer for help with the RT-PCR experiments and helpful comments on the manuscript, and to Dr. Juan Archelos for providing the P07 antibody. We thank Eva Kronberg for animal care and Heinrich Blazyca for excellent technical assistance (tissue processing for light and electron microscopy).

This work is supported by the Deutsche Forschungsgemeinschaft (SFB 581, Priority Program "Microglia" MA1053/3, to R. Martini) and by the Gemeinnützige Hertie-Stiftung (to M. Schachner and R. Martini).

Submitted: 17 February 2004
Accepted: 19 April 2004

References

Adlkofer, K., R. Martini, A. Aguzzi, J. Zielasek, K.V. Toyka, and U. Suter. 1995. Hypermyelination and demyelinating peripheral neuropathy in Pmp22-deficient mice. *Nat. Genet.* 11:274–280.

Adlkofer, K., R. Frei, D.H. Neuberg, J. Zielasek, K.V. Toyka, and U. Suter. 1997. Heterozygous peripheral myelin protein 22-deficient mice are affected by a progressive demyelinating tomaculous neuropathy. *J. Neurosci.* 17:4662–4671.

Archelos, J.J., K. Roggenbuck, J. Schneider-Schaulies, C. Linington, K.V. Toyka, and H.P. Hartung. 1993. Production and characterization of monoclonal antibodies to the extracellular domain of P0. *J. Neurosci. Res.* 35:46–53.

Bennett, C.L., and P.F. Chance. 2001. Molecular pathogenesis of hereditary motor, sensory and autonomic neuropathies. *Curr. Opin. Neurol.* 14:621–627.

Boerkoel, C.F., H. Takashima, P. Stankiewicz, C.A. Garcia, S.M. Leber, L. Rhee-Morris, and J.R. Lupski. 2001. Periaxin mutations cause recessive Dejerine-Sottas neuropathy. *Am. J. Hum. Genet.* 68:325–333.

Cai, Z., K. Cash, J. Swift, P. Sutton-Smith, M. Robinson, P.D. Thompson, and P.C. Blumbergs. 2001. Focal myelin swellings and tomacula in anti-MAG IgM paraproteinaemic neuropathy: novel teased nerve fiber studies. *J. Peripher. Nerv. Syst.* 6:95–101.

Cai, Z., P. Sutton-Smith, J. Swift, K. Cash, J. Finnie, A. Turnley, P.D. Thompson, and P.C. Blumbergs. 2002. Tomacula in MAG-deficient mice. *J. Peripher. Nerv. Syst.* 7:181–189.

Carenini, S., D. Montag, H. Cremer, M. Schachner, and R. Martini. 1997. Absence of the myelin-associated glycoprotein (MAG) and the neural cell adhesion molecule (N-CAM) interferes with the maintenance, but not with the formation of peripheral myelin. *Cell Tissue Res.* 287:3–9.

Carenini, S., M. Maurer, A. Werner, H. Blazyca, K.V. Toyka, C.D. Schmid, G. Raivich, and R. Martini. 2001. The role of macrophages in demyelinating peripheral nervous system of mice heterozygously deficient in P0. *J. Cell Biol.* 152:301–308.

D'Urso, D., P. Ehrhardt, and H.W. Muller. 1999. Peripheral myelin protein 22 and protein zero: a novel association in peripheral nervous system myelin. *J. Neurosci.* 19:3396–3403.

Dyck, P.J., P. Chance, R. Lebo, and J.A. Carney. 1993. Hereditary motor and sensory neuropathies. *In* Peripheral Neuropathy, 3rd ed. P.J. Dyck, P.K. Thomas, J.W. Griffin, P.A. Low, and J.F. Poduslo, editors. W.B. Saunders, Philadelphia. 1094–1136.

Fabrizi, G.M., F. Taioli, T. Cavallaro, F. Rigatelli, A. Simonati, G. Mariani, P. Perrone, and N. Rizzuto. 2000. Focally folded myelin in Charcot-Marie-Tooth neuropathy type 1B with Ser49Leu in the myelin protein zero. *Acta Neuropathol. (Berl.).* 100:299–304.

Feltri, M.L., M. D'Antonio, A. Quattrini, R. Numerato, M. Arona, S. Previtali, S.Y. Chiu, A. Messing, and L. Wrabetz. 1999. A novel P0 glycoprotein transgene activates expression of lacZ in myelin-forming Schwann cells. *Eur. J. Neurosci.* 11:1577–1586.

Friede, R.L. 1972. Control of myelin formation by axon caliber (with a model of the control mechanism). *J. Comp. Neurol.* 144:233–252.

Gabreëls-Festen, A.A., E.M. Joosten, F.J. Gabreels, D.F. Stegeman, A.J. Vos, and

H.F. Busch. 1990. Congenital demyelinating motor and sensory neuropathy with focally folded myelin sheaths. *Brain.* 113:1629–1643.

Gabreëls-Festen, A.A., J.E. Hoogendijk, P.H. Meijerink, F.J. Gabreëls, P.A. Bolhuis, S. van Beersum, T. Kulkens, E. Nelis, F.G. Jennekens, M. de Visser, et al. 1996. Two divergent types of nerve pathology in patients with different P0 mutations in Charcot-Marie-Tooth disease. *Neurology.* 47:761–765.

Giese, K.P., R. Martini, G. Lemke, P. Soriano, and M. Schachner. 1992. Mouse P0 gene disruption leads to hypomyelination, abnormal expression of recognition molecules, and degeneration of myelin and axons. *Cell.* 71:565–576.

Gillespie, C.S., D.L. Sherman, S.M. Fleetwood-Walker, D.F. Cottrell, S. Tait, E.M. Garry, V.C. Wallace, J. Ure, I.R. Griffiths, A. Smith, and P.J. Brophy. 2000. Peripheral demyelination and neuropathic pain behavior in periaxin-deficient mice. *Neuron.* 26:523–531.

Guilbot, A., A. Williams, N. Ravise, C. Verny, A. Brice, D.L. Sherman, P.J. Brophy, E. LeGuern, V. Delague, C. Bareil, et al. 2001. A mutation in periaxin is responsible for CMT4F, an autosomal recessive form of Charcot-Marie-Tooth disease. *Hum. Mol. Genet.* 10:415–421.

Hayasaka, K., M. Himoro, W. Sato, G. Takada, K. Uyemura, N. Shimizu, T.D. Bird, P.M. Conneally, and P.F. Chance. 1993a. Charcot-Marie-Tooth neuropathy type 1B is associated with mutations of the myelin P0 gene. *Nat. Genet.* 5:31–34.

Hayasaka, K., M. Himoro, Y. Sawaishi, K. Nanao, T. Takahashi, G. Takada, G.A. Nicholson, R.A. Ouvrier, and N. Tachi. 1993b. De novo mutation of the myelin P0 gene in Dejerine-Sottas disease (hereditary motor and sensory neuropathy type III). *Nat. Genet.* 5:266–268.

Hayasaka, K., G. Takada, and V.V. Ionasescu. 1993c. Mutation of the myelin P0 gene in Charcot-Marie-Tooth neuropathy type 1B. *Hum. Mol. Genet.* 2:1369–1372.

Hogan, B., R. Beddington, F. Constantini, and E. Lacy. 1994. Manipulating the Mouse Embryo. Cold Spring Harbor Laboratory Press, Cold Spring Harbor, NY. 497 pp.

Inoue, H., H. Tsuruta, J. Sedzik, K. Uyemura, and D.A. Kirschner. 1999. Tetrameric assembly of full-sequence protein zero myelin glycoprotein by synchrotron X-ray scattering. *Biophys. J.* 76:423–437.

Kamholz, J., D. Menichella, A. Jani, J. Garbern, R.A. Lewis, K.M. Krajewski, J. Lilien, S.S. Scherer, and M.E. Shy. 2000. Charcot-Marie-Tooth disease type 1: molecular pathogenesis to gene therapy. *Brain.* 123:222–233.

Kirschner, D.A., and R.A. Saavedra. 1994. Mutations in demyelinating peripheral neuropathies support molecular model of myelin P0-glycoprotein extracellular domain. *J. Neurosci. Res.* 37:574–583.

Kobsar, I., M. Berghoff, M. Samsam, C. Wessig, M. Maurer, K.V. Toyka, and R. Martini. 2003. Preserved myelin integrity and reduced axonopathy in connexin32-deficient mice lacking the recombination activating gene-1. *Brain.* 126:804–813.

Kulkens, T., P.A. Bolhuis, R.A. Wolterman, S. Kemp, S. te Nijenhuis, L.J. Valentijn, G.W. Hensels, F.G. Jennekens, M. de Visser, J.E. Hoogendijk, and F. Baas. 1993. Deletion of the serine 34 codon from the major peripheral myelin protein P0 gene in Charcot-Marie-Tooth disease type 1B. *Nat. Genet.* 5:35–39.

Lemke, G., E. Lamar, and J. Patterson. 1988. Isolation and analysis of the gene encoding peripheral myelin protein zero. *Neuron.* 1:73–83.

Lindberg, R.L.P., R. Martini, M. Baumgartner, B. Erne, J. Borg, J. Zielasek, K. Ricker, A. Steck, K.V. Toyka, and U.A. Meyer. 1999. Motor neuropathy in porphobilinogen deaminase-deficient mice imitates the peripheral neuropathy of human acute porphyria. *J. Clin. Invest.* 103:1127–1134.

Martini, R. 1994. Expression and functional roles of neural cell surface molecules and extracellular matrix components during development and regeneration of peripheral nerves. *J. Neurocytol.* 23:1–28.

Martini, R. 1999. P0-deficient knockout mice as tools to understand pathomechanisms in Charcot-Marie-Tooth 1B and P0-related Dejerine-Sottas syndrome. *Ann. NY Acad. Sci.* 883:273–280.

Martini, R., and M. Schachner. 1997. Molecular bases of myelin formation as revealed by investigations on mice deficient in glial cell surface molecules. *Glia.* 19:298–310.

Martini, R., M.H. Mohajeri, S. Kasper, K.P. Giese, and M. Schachner. 1995a. Mice doubly deficient in the genes for P0 and myelin basic protein show that both proteins contribute to the formation of the major dense line in peripheral nerve myelin. *J. Neurosci.* 15:4488–4495.

Martini, R., J. Zielasek, K.V. Toyka, K.P. Giese, and M. Schachner. 1995b. Protein zero (P0)-deficient mice show myelin degeneration in peripheral nerves characteristic of inherited human neuropathies. *Nat. Genet.* 11:281–286.

Martini, R., J. Zielasek, and K.V. Toyka. 1998. Inherited demyelinating neuropathies: from gene to disease. *Curr. Opin. Neurol.* 11:545–556.

Menichella, D.M., E.J. Arroyo, R. Awatramani, T. Xu, P. Baron, J.M. Vallat, J. Balsamo, J. Lilien, G. Scarlato, J. Kamholz, et al. 2001. Protein zero is necessary for E-cadherin-mediated adherens junction formation in Schwann cells. *Mol. Cell. Neurosci.* 18:606–618.

Nakagawa, M., M. Suehara, A. Saito, H. Takashima, F. Umehara, M. Saito, N. Kanzato, T. Matsuzaki, S. Takenaga, S. Sakoda, et al. 1999. A novel MPZ gene mutation in dominantly inherited neuropathy with focally folded myelin sheaths. *Neurology.* 52:1271–1275.

Rebai, T., C. Mhiri, P. Heine, H. Charfi, C. Meyrignac, and R. Gherardi. 1989. Focal myelin thickenings in a peripheral neuropathy associated with IgM monoclonal gammopathy. *Acta Neuropathol. (Berl.).* 79:226–232.

Schneider-Schaulies, J., A. von Brunn, and M. Schachner. 1990. Recombinant peripheral myelin protein P0 confers both adhesion and neurite outgrowth-promoting properties. *J. Neurosci. Res.* 27:286–297.

Shapiro, L., J.P. Doyle, P. Hensley, D.R. Colman, and W.A. Hendrickson. 1996. Crystal structure of the extracellular domain from P0, the major structural protein of peripheral nerve myelin. *Neuron.* 17:435–449.

Shy, M.E., J.Y. Garbern, and J. Kamholz. 2002. Hereditary motor and sensory neuropathies: a biological perspective. *Lancet Neurol.* 1:110–118.

Sindou, P., J.-M. Vallat, F. Chapon, J. Archelos, F. Tabaraud, T. Anani, K. Braund, T. Maisonobe, J.-J. Hauw, and A. Vandenberghe. 1999. Ultrastructural protein zero expression in Charcot-Marie-Tooth type 1B disease. *Muscle Nerve.* 22:99–104.

Suter, U., and K.A. Nave. 1999. Transgenic mouse models of CMT1A and HNPP. *Ann. NY Acad. Sci.* 883:247–253.

Tachi, N., N. Kozuka, K. Ohya, S. Chiba, and K. Sasaki. 1997. Tomaculous neuropathy in Charcot-Marie-Tooth disease with myelin protein zero gene mutation. *J. Neurol. Sci.* 153:106–109.

Takashima, H., C.F. Boerkoel, P. De Jonghe, C. Ceuterick, J.J. Martin, T. Voit, J.M. Schroder, A. Williams, P.J. Brophy, V. Timmerman, and J.R. Lupski. 2002. Periaxin mutations cause a broad spectrum of demyelinating neuropathies. *Ann. Neurol.* 51:709–715.

Thomas, F.P., R.V. Lebo, G. Rosoklija, X.S. Ding, R.E. Lovelace, N. Latov, and A.P. Hays. 1994. Tomaculous neuropathy in chromosome 1 Charcot-Marie-Tooth syndrome. *Acta Neuropathol. (Berl.).* 87:91–97.

Warner, L.E., M.J. Hilz, S.H. Appel, J.M. Killian, E.H. Kolodry, G. Karpati, S. Carpenter, G.V. Watters, C. Wheeler, D. Witt, et al. 1996. Clinical phenotypes of different MPZ (P0) mutations may include Charcot-Marie-Tooth type 1B, Dejerine-Sottas, and congenital hypomyelination. *Neuron.* 17:451–460.

Wrabetz, L., M.L. Feltri, A. Quattrini, D. Imperiale, S. Previtali, M. D'Antonio, R. Martini, X. Yin, B.D. Trapp, L. Zhou, et al. 2000. P(0) glycoprotein overexpression causes congenital hypomyelination of peripheral nerves. *J. Cell Biol.* 148:1021–1034.

Yin, X., G.J. Kidd, L. Wrabetz, M.L. Feltri, A. Messing, and B.D. Trapp. 2000. Schwann cell myelination requires timely and precise targeting of P0 protein. *J. Cell Biol.* 148:1009–1020.

You, K.H., C.L. Hsieh, C. Hayes, N. Stahl, U. Francke, and B. Popko. 1991. DNA sequence, genomic organization, and chromosomal localization of the mouse peripheral myelin protein zero gene: identification of polymorphic alleles. *Genomics.* 9:751–757.

Young, P., and U. Suter. 2001. Disease mechanisms and potential therapeutic strategies in Charcot-Marie-Tooth disease. *Brain Res. Brain Res. Rev.* 36: 213–221.

Young, P., and U. Suter. 2003. The causes of Charcot-Marie-Tooth disease. *Cell. Mol. Life Sci.* 60:2547–2560.

Zielasek, J., M. Martini, and K.V. Toyka. 1996. Functional abnormalities in P0-deficient mice resemble human hereditary neuropathies linked to P0 gene mutations. *Muscle Nerve.* 19:946–952.